Journal of Southeast University (English Edition) Vol. 40, No. 4, pp. 403 – 409 Dec. 2024 ISSN 1003—7985

Electrical power generator from electrospun hybrid PVDF-$BaTiO_3$ nanofiber membranes

Zhou Lei[1] Zhou Hexiang[2] Ma Jian[2,3]

([1]College of Communication and Art Design, University of Shanghai for Science and Technology, Shanghai 200093, China)
([2]School of Mechanical Engineering, Southeast University, Nanjing 211189, China)
([3]Engineering Research Center of New Light Sources Technology and Equipment of Ministry of Education, Southeast University, Nanjing 211189, China)

Abstract: To enhance the piezoelectric performance of piezoelectric polymer thin films in general, hybrid polyvinylidene difluoride (PVDF) and nanosized barium titanate ($BaTiO_3$) piezoelectric films were prepared and their piezoelectric performance examined. The hybrid nanofibers were fabricated via electrospinning at an external voltage of 15 kV. The nonwoven fabrics were collected using a roller collection device, and their morphological structures were analyzed via scanning electron microscopy. The crystal structures of these piezoelectric films were characterized via micro-Raman spectroscopy. β-phase of the composite nanofiber membrane almost increased to twice owing to the addition of $BaTiO_3$ nanoparticles. Compared with pure, electrospun PVDF piezoelectric film, the piezoelectric characteristics of the hybrid piezoelectric films were considerably enhanced because of the additional $BaTiO_3$ nanoparticles. The maximum instantaneous open-circuit voltage of the hybrid PVDF-$BaTiO_3$ nanofibers film can be high up to 80 V. The high-performance hybrid piezoelectric films exhibited notable prospects for applications in wearable electronic textiles.

Key words: electrospinning; polyvinylidene difluoride (PVDF) nanofiber; barium titanate ($BaTiO_3$); piezoelectric film

DOI: 10.3969/j.issn.1003 – 7985.2024.04.009

With the development of portable and wearable devices for human health control and monitoring, the progress in the field of flexible, lightweight, and small self-powering sources has been rapid[1–4]. Piezoelectric materials are one of the most important materials used for energy harvesting, and many studies have been conducted on them. They are suitable for self-powering generators because they can generate electricity via deformations due to small forces from tensile stress, mechanical impact, mechanical vibration, bending, and pressure[5–8]. The most common piezoelectric materials, such as piezoelectric ceramics[9], have relatively satisfactory piezoelectric properties; however, their application in wearable devices is difficult because of their brittleness and rigidity. Another group of piezoelectric materials is semiconductor nanowires, such as those made of ZnO[10–13], InN[14], GaN[15–16], CdS[17–18], and ZnS[19]. These piezoelectric nanowires have demonstrated a notable ability to convert mechanical vibrations into electrical energy. However, these nanowires typically must be combined with organic compounds prior to application in wearable devices. Furthermore, polymer piezoelectric materials are another type of piezoelectric materials. Polymer films have higher flexibility than inorganic thin film materials[20–22]. Polyvinylidene difluoride (PVDF) is considered one of the most popular piezoelectric polymers because of its relatively large piezoelectric coefficients, attractive mechanical properties, ease of processing, chemical stability, and biocompatibility[23–30]. These features make PVDF particularly attractive for wearable and implantable energy-harvesting devices.

The piezoelectric properties of PVDF considerably depend on its crystalline phases. PVDF possesses five different crystalline phases, mainly because its simple chemical structure with alternating CH_2 and CF_2 groups can result in various polycrystalline orientations depending on processing conditions. Various chain conformations correspond to the five crystalline phases: α, β, γ, δ, and ε, depending on the chain conformation of trans (T) and gauche (G) linkages[31–36]. Of the five polymorphs, β-phase exhibits the highest piezo-, pyro-, and ferroelectric properties. This is because of its polar structure with oriented hydrogen and fluoride unit cells along the carbon backbone. Thus, several approaches have been used in the literature to enhance the transformation of β-phase in a bid to obtain piezoelectric PVDF: application of high electric field, mechanical stretching, drawing, casting, epitaxy process, and doping with organic and inorganic materials, etc.[37]. Electrospinning is one of the simplest methods to fabricate high β-phase PVDF.

Received 2024-03-11, **Revised** 2024-05-17.

Biographies: Zhou Lei (1985—), female, doctor, associate professor; Ma Jian (corresponding author) male, doctor, associate professor, jian.ma@seu.edu.cn.

Foundation items: The National Natural Science Foundation of China (No. 52375563), the Science and Technology on Avionics Integration Laboratory (No. 201913069001, 20200055069001).

Citation: Zhou Lei, Zhou Hexiang, Ma Jian. Electrical power generator from electrospun hybrid PVDF-$BaTiO_3$ nanofiber membranes[J]. Journal of Southeast University (English Edition), 2024, 40(4): 403 – 409. DOI: 10.3969/j.issn.1003 – 7985.2024.04.009.

Electrospinning is a versatile process that can be used to fabricate polymer nanofibers from various materials. During electrospinning, polymer molecules are typically stretched and arranged along the fiber axis because of the strong elongation flow in the jet. Many studies have shown that electrospinning can transform the nonpolar α-phase PVDF to the polar β-phase material, resulting in piezoelectric nanofibers[38-40]. Near-field electrospinning can be used to fabricate piezoelectric PVDF nanofibers on working substrates via in situ mechanical stretching and electrical poling[23,27,41]. Damaraju et al.[34] observed that increasing electrospinning voltage resulted in increased β-phase fraction. They reported an optimized electrospinning voltage of 25 kV to achieve the highest β-phase fraction. In addition, incorporating nanomaterials during the electrospinning process can also increase β-phase fraction. Yu et al.[42] observed that adding 5% multiwalled carbon nanotubes (MWCNTs) to the PVDF electrospinning solution increased both the crystallinity and proportion of β-phase. With additional MWCNTs, the surface conductivity of PVDF nanofiber mats increased, which is believed to further increase the output power. Athira et al.[28] also observed that upon the addition of 10% $BaTiO_3$ nanoparticles, the electroactive β-phase of the PVDF increased in proportion to about 91% as a result of the synergistic interfacial interaction between the tetragonal $BaTiO_3$ nanoparticles and ferroelectric host polymer matrix upon electrospinning. All the above-mentioned methods can be used to increase β-phase fraction.

The piezoelectric performance of PVDF is determined by its piezoelectric voltage constant (g_{33}) and dielectric constant (d_{33}). As is known, PVDF has high g_{33} but considerably low d_{33}[43]. Several studies have reported that introducing high dielectric constant piezoelectric material filler into PVDF matrix can increase the dielectric constant of PVDF; nanoparticles such as carbon nanotubes, graphene, BaTiO, and ZnO have been used most of the time to realize this improvement. Lee et al.[44] fabricated a highly sensitive and multifunctional sensor using a PVDF/ZnO nanorod composite thin film. In addition, they demonstrated hybrid fiber generators consisting of ZnO nanowires and PVDF infiltrating polymer[45]. Li et al.[46] also demonstrated a novel generator film comprising hybrid PVDF and ZnO nanowires; it was suggested that the ZnO nanowires served not only as a piezoelectric material but also as an additive that facilitated the formation of β-phase and the stability of the PVDF film by stretching and increasing the contact surface area.

In this study, PVDF-$BaTiO_3$ composite nanofibers were fabricated via electrospinning and collected via a drum-type collector. $BaTiO_3$ is considered the most environmentally friendly material, and it also exhibits high piezoelectric and ferroelectric characteristics along with a high dielectric constant. Nanofibers collected by the drum collector have high orderliness compared with those without drum collector. To investigate the effect of added nanoparticles on the microstructure of PVDF nanofibers, micro-Raman spectroscopy was conducted to measure the relative fraction of β-phase PVDF in individual hybrid and pure nanofibers, respectively. By comparing the energy-harvesting efficiency of PVDF-$BaTiO_3$ hybrid nanofibers with that of pure PVDF nanofibers, we observed that the added nanoparticles not only facilitated the formation of β-phase but also enhanced their piezoelectric characteristics.

1 Fabrication of Nanofibers

Fig. 1 shows the electrospinning setup for fabricating PVDF-$BaTiO_3$ hybrid nanofibers. To prevent $BaTiO_3$ nanoparticles from clustering in the PVDF solution, 10% $BaTiO_3$ nanoparticles were first ultrasonically dispersed in N, N-dimethylformamide solution for 12 h. Thereafter, the PVDF powder was dissolved in the mixture solution, followed by stirring with a high-speed magnetic stirrer until complete dissolution. The molecular weight of the PVDF powder was about 1.2×10^5. All these experimental supplies were purchased from Sigma. The mixed solution was stirred at 80 ℃ to expedite the dissolution. Pure PVDF solution was also separately prepared at the same weight concentration for comparison with hybrid PVDF-$BaTiO_3$ nanofibers. During the electrospinning process, a 5-mL syringe was used to draw the polymer solution. A 0.4 mm × 25 mm metal needle was connected to the end of the syringe reservoir. The syringe was mounted on a syringe pump, which provided a constant flow rate of 10

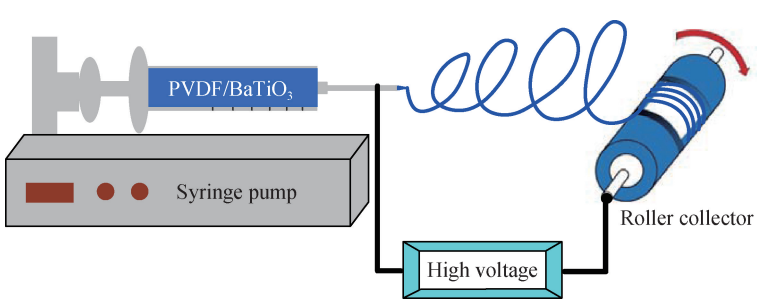

Fig. 1 Electrospinning-aligned PVDF and $BaTiO_3$ nanofiber film with the roller collector

μL/min. Electrospinning was conducted at 15 kV, with a constant distance of 150 mm between the tip of the spinneret and the collector. The high voltage was supplied by an EMCO DX250 DC-DC converter. A roller collector with a rotation speed maintained at 300 r/min was used to obtain aligned nanofibers. The films used for the piezoelectric performance test were obtained via electrospinning with 10 mL of the polymer solution.

The morphology of the nanofibers was characterized using an FEI-Helios NanoLab 600i instrument. The Raman spectra of PVDF and hybrid PVDF-$BaTiO_3$ nanofibers were collected from the nanofiber film at room temperature via 10-mW laser radiation at 532 nm. The spectra were accumulated for 3 min and taken with a slit width equivalent to 1.5 cm^{-1} resolution using the Alpha300 R WITec system.

2 Nanofiber Characterization Experiment

2.1 Morphological characterization of nanofibers

Fig. 2(a) shows a scanning electron microscopy image of pure PVDF nanofibers electrospun at 15% concentration and collected using an ordinary flat collector. The surface is smooth, and the average diameter range of the nanofibers is about 200 nm. Compared with disordered nanofibers, Fig. 2(b) shows the aligned PVDF nanofibers collected using the roller collector. Clearly, the arrangement of nanofibers obtained by the roller receiver is more orderly than that of those collected using the flat collector. Fig. 2(c) shows hybrid PVDF-$BaTiO_3$ nanofibers also collected using the roller collector. $BaTiO_3$ nanoparticles can be clearly observed from the surface of the nanofibers, and the distribution of the nanoparticles is relatively uniform without serious agglomeration phenomenon. This is attributed to the ultrasonic vibration of $BaTiO_3$ nanoparticles during the preparation of the organic solution. During the experiment, we observed that the nanofibers obtained via electrospinning were discontinuous, even beady, if the PVDF concentration was lower than 15%.

2.2 Characterization of nanofiber crystal structure

Fig. 3(a) shows the Raman spectra recorded using the 532-nm laser line for each of the PVDF powder, pure PVDF nanofibers, and hybrid PVDF-$BaTiO_3$ nanofibers. The Raman characteristic peaks of α-phase PVDF are mainly manifested at 276, 413, 609, and 794 cm^{-1}, as shown in Fig. 3(a) for PVDF powder. However, the Raman characteristic peaks of β-phase PVDF are mainly manifested at 510 and 839 cm^{-1}. The transition from α-phase to β-phase can be monitored by comparing the relative intensities of the bands at 794(indicative of α-phase) and 839 cm^{-1}(indicative of β-phase)[32–33]. In the Raman spectra of PVDF powder, the relative intensity of the band at 794 cm^{-1} was considerably higher than that of the band at 839 cm^{-1} (indicating a predominance of α-phase), as shown in Fig. 3(a). However, this relationship is reversed in the Raman spectra of electrospun PVDF nanofibers (indicating a considerable increase in β-phase content) in Fig. 3(b). This transformation occurred because the molecular chains of PVDF powder were straightened and polarized under high voltage during the electrospinning process. The same transformation can be observed from the Raman spectra of hybrid PVDF-$BaTiO_3$ nanofibers.

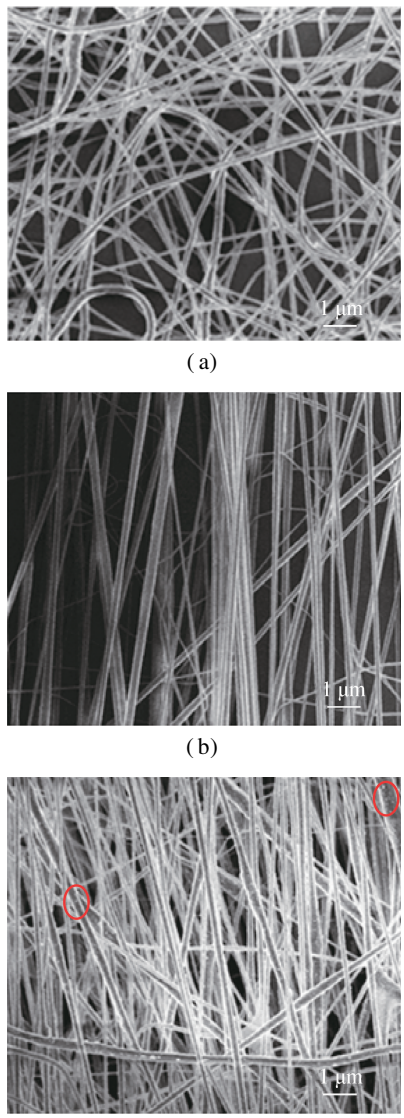

Fig. 2 Scanning electron microscopy image of electrospun nanofibers. (a) Disordered PVDF nanofibers; (b) Aligned PVDF nanofibers; (c) Hybrid PVDF-$BaTiO_3$ nanofibers

Compared with pure PVDF nanofibers, the intensity ratio of the β-phase peak (839 cm^{-1}) to the α-phase peak (794 cm^{-1}) considerably increased from 1.5 to 2.6 for the hybrid PVDF-$BaTiO_3$ nanofibers. This indicates that the addition of $BaTiO_3$ nanoparticles increased the fraction of β-phase. This increase is attributed to the interactions at the surface of the nanoparticles. The hydrogen of the

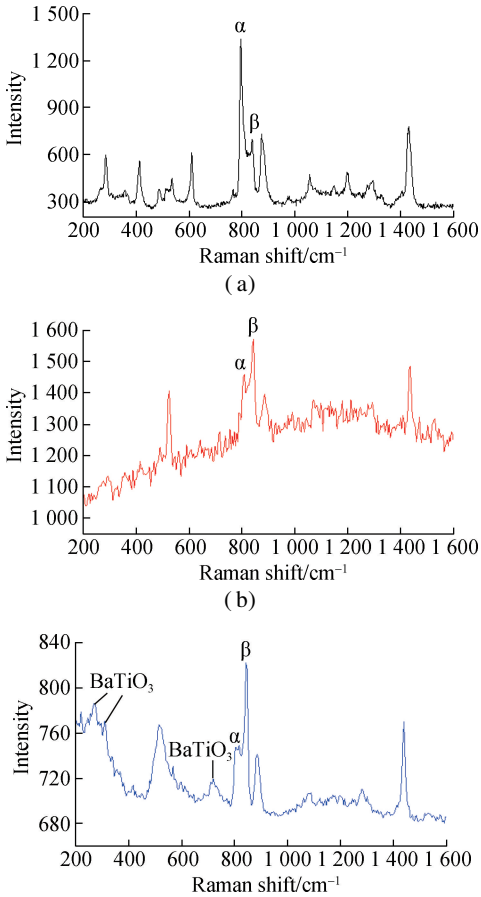

Fig. 3 Raman spectra of various samples. (a) PVDF powder; (b) PVDF nanofibers; (c) Hybrid PVDF-$BaTiO_3$ nanofibers

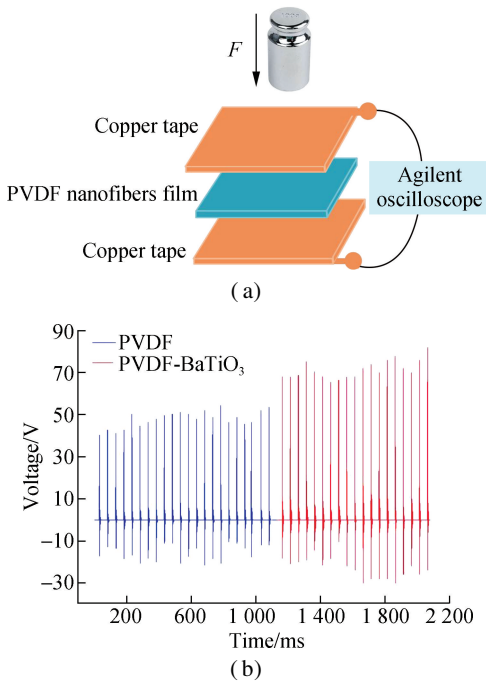

Fig. 4 Measurement of piezoelectric performance. (a) Output voltage test; (b) Output voltage result

carboxyl group on the nanoparticle surface is hydrogen bonded to the fluorine of the polymer chain, and it forms CH_2/CF_2 dipoles. These interactions result in the formation of β-phase crystals with an all-trans conformation in the polymer chain. Conversely, nanoparticles act as the nucleating agent of β-phase. The Raman characteristic peaks of $BaTiO_3$ nanofibers at 265, 305, and 720 cm^{-1} also can be observed for the hybrid nanofibers, as shown in Fig. 3(c).

2.3 Piezoelectric output voltage experiment

A piezoelectric performance measurement circuit was designed for the prepared nanofibrous membrane, and it was packaged in patches, as shown in Fig. 4(a). The piezoelectric nanogenerator film was sandwiched by two layers of conductive copper tapes. A force was applied to all samples with a period of 50 ms. An oscilloscope screen image representing the amount of the cyclic force and the output voltage of PVDF is shown in Fig. 4(b).

The maximum output voltage of the two piezoelectric films was measured by gradually increasing the pressure, as shown in Fig. 4(b). After repeated measurements, the maximum instantaneous open-circuit voltage peak of the PVDF piezoelectric film was stable at 40-55 V, and that of the composite PVDF-$BaTiO_3$ piezoelectric film was stable at 65-80 V. The addition of $BaTiO_3$ increased the output voltage of the piezoelectric thin films by almost twice. This increase can be explained as follows. Firstly, from the Raman spectra results, we confirmed that the addition of $BaTiO_3$ nanoparticles can result in more PVDF domains transitioning from α-phase to β-phase owing to the synergistic interfacial interaction between the tetragonal $BaTiO_3$ nanoparticles and the ferroelectric host polymer matrix upon electrospinning[28]. Secondly, the roller collector makes the distribution of PVDF nanofibers obtained more orderly, resulting in higher output voltage.

From Fig. 4(b), one can see that the output voltage is positive when pressure acts on the thin film, and the output voltage is negative when pressure is withdrawn, similar to pulse voltage, which cannot be directly used for energy storage. We designed a circuit to further store the output energy of the piezoelectric film, as shown in Fig. 5(a). The piezoelectric film is used to charge the Faraday capacitor, which then discharges the load upon reaching its rated voltage. By using AC and DC, the capacitor can be charged twice in a single cycle by using a traditional bridge rectifier circuit. The small capacitor is first charged and discharged to the Faraday capacitor after reaching the rated voltage value. This reduces the resistance and power of the current limiting resistor R_b as well as the power loss during charging, and this also effectively avoids the reduction in power extraction efficiency of the online power supply because of the reduction in terminal voltage (see Fig. 5(a)).

The charging time of two types of piezoelectric thin films

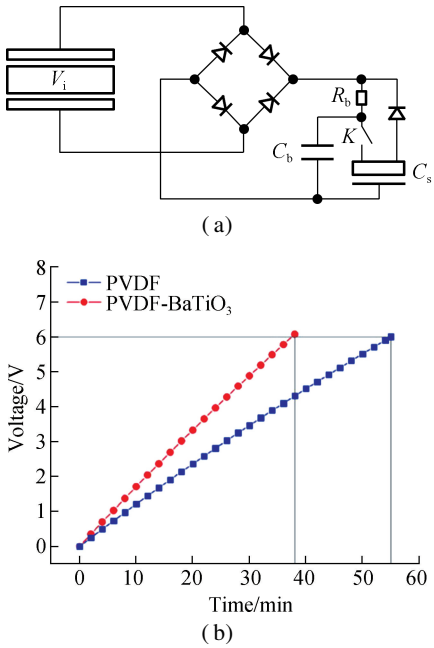

Fig. 5 Simulation of the piezoelectric thin film circuit. (a) Energy storage circuit; (b) Charging simulation results

was simulated to compare their energy supply capacity. The capacitance value used in the simulation was 0.47 F, and the rated voltage of the Faraday capacitor was 6.0 V. The input voltage was derived from the open-circuit voltage waveform of the piezoelectric film, characterized by a 50 ms cycle, with a rise time of 2 ms and a fall time of 2 ms. The peak voltages were 60 and 80 V for the PVDF piezoelectric film and composite PVDF-$BaTiO_3$ piezoelectric film, respectively. These simulations are conducted under high-frequency pressure applied to the films during the capacitance charging process. The Faraday capacitor voltage varied with time, as shown in Fig. 5(b). The charging time of the composite piezoelectric film (37 min) was reduced by approximately 18 min compared with the PVDF piezoelectric film (55 min). In the practical application of the energy storage circuit, the resistance of piezoelectric film must be considered, which has been ignored in this study. Reducing the internal resistance is also highly important to increase the energy supply efficiency of the piezoelectric film.

3 Conclusions

1) PVDF thin films and composite PVDF-$BaTiO_3$ films, both prepared via electrospinning, exhibited remarkable piezoelectric characteristics and had more potential to be explored compared with traditional piezoelectric ceramics.

2) The strong electric fields and stretching forces from the electrospinning process naturally aligned dipoles in the PVDF nanofiber crystal, such that the nonpolar α-phase (random orientation of dipoles) was transformed into the polar β-phase, determining the polarity of the electrospun nanofibers. The proportion of crystal-structure β-phase of the PVDF fibers also increased because of the addition of $BaTiO_3$ nanowires.

3) The addition of $BaTiO_3$ nanoparticles increased the piezoelectric coefficient of the entire PVDF material. The maximum output voltage generated by hybrid PVDF-$BaTiO_3$ nanofibers (10% $BaTiO_3$ nanoparticles) was almost twice the voltage produced by pure, electrospun PVDF nanofibers. Piezoelectric films have been witnessing a broad market with the rapid development of low-power wearable devices. Accordingly, high-performance piezoelectric films can also form the basis for the development of flexible, smart, wearable piezoelectric sensor devices.

References

[1] Zhao Z, Dai Y, Dou S X, et al. Flexible nanogenerators for wearable electronic applications based on piezoelectric materials [J]. *Materials Today Energy*, 2021, **20**: 100690. DOI: 10.1016/j.mtener.2021.100690.

[2] Xu C, Song Y, Han M D, et al. Portable and wearable self-powered systems based on emerging energy harvesting technology[J]. *Microsystems & Nanoengineering*, 2021, **7**: 25. DOI: 10.1038/s41378-021-00248-z.

[3] Nan X L, Wang X, Kang T T, et al. Review of flexible wearable sensor devices for biomedical application [J]. *Micromachines*, 2022, **13**(9): 1395. DOI: 10.3390/mi13091395.

[4] Liu L M, Zhang H J, Zhou S Y, et al. Boosting the piezoelectric response and interfacial compatibility in flexible piezoelectric composites via DET-doping BT nanoparticles [J]. *Polymers*, 2024, **16**(6): 743. DOI: 10.3390/polym16060743.

[5] Sorayani Bafqi M S, Bagherzadeh R, Latifi M. Fabrication of composite PVDF-ZnO nanofiber mats by electrospinning for energy scavenging application with enhanced efficiency[J]. *Journal of Polymer Research*, 2015, **22**(7): 130. DOI: 10.1007/s10965-015-0765-8.

[6] Serairi L, Leprince-Wang Y. ZnO nanowire-based piezoelectric nanogenerator device performance tests[J]. *Crystals*, 2022, **12**(8): 1023. DOI: 10.3390/cryst12081023.

[7] Lopez Garcia A J, Mouis M, Cresti A, et al. Influence of slow or fast surface traps on the amplitude and symmetry of the piezoelectric response of semiconducting-nanowire-based transducers [J]. *Journal of Physics D: Applied Physics*, 2022, **55**(40): 405502. DOI: 10.1088/1361-6463/ac8251.

[8] Hao F Q, Wang B, Wang X, et al. Soybean-inspired nanomaterial-based broadband piezoelectric energy harvester with local bistability [J]. *Nano Energy*, 2022, **103**: 107823. DOI: 10.1016/j.nanoen.2022.107823.

[9] Chen K H, Cheng C M, Chen Y J, et al. Lead-free piezoelectric ceramic micro-pressure thick films[J]. *Crystals*, 2023, **13**(2): 201. DOI: 10.3390/cryst13020201.

[10] Wang Z L, Song J H. Piezoelectric nanogenerators based on zinc oxide nanowire arrays[J]. *Science*, 2006, **312**(5771): 242-246. DOI: 10.1126/science.1124005.

[11] Qin Y, Wang X D, Wang Z L. Microfibre-nanowire hybrid structure for energy scavenging[J]. *Nature*, 2008,

451(7180): 809 - 813. DOI: 10.1038/nature06601.

[12] Zhu G, Yang R S, Wang S H, et al. Flexible high-output nanogenerator based on lateral ZnO nanowire array[J]. *Nano Letters*, 2010, **10**(8): 3151 - 3155. DOI: 10.1021/nl101973h.

[13] Hu Y F, Lin L, Zhang Y, et al. Replacing a battery by a nanogenerator with 20 V output[J]. *Advanced Materials*, 2012, **24**(1): 110 - 114. DOI: 10.1002/adma.201103727.

[14] Huang C T, Song J H, Tsai C M, et al. Single-InN-nanowire nanogenerator with upto 1 V output voltage[J]. *Advanced Materials*, 2010, **22**(36): 4008 - 4013. DOI: 10.1002/adma.201000981.

[15] Huang C T, Song J H, Lee W F, et al. GaN nanowire arrays for high-output nanogenerators[J]. *Journal of the American Chemical Society*, 2010, **132**(13): 4766 - 4771. DOI: 10.1021/ja909863a.

[16] Wang X B, Song J H, Zhang F, et al. Electricity generation based on one-dimensional group-Ⅲ nitride nanomaterials[J]. *Advanced Materials*, 2010, **22**(19): 2155 - 2158. DOI: 10.1002/adma.200903442.

[17] Lin Y F, Song J H, Ding Y, et al. Piezoelectric nanogenerator using CdS nanowires[J]. *Applied Physics Letters*, 2008, **92**(2): 022105. DOI: 10.1063/1.2831901.

[18] Lin Y F, Song J H, Ding Y, et al. Alternating the output of a CdS nanowire nanogenerator by a white-light-stimulated optoelectronic effect[J]. *Advanced Materials*, 2008, **20**(16): 3127 - 3130. DOI: 10.1002/adma.200703236.

[19] Lu M Y, Song J H, Lu M P, et al. ZnO-ZnS heterojunction and ZnS nanowire arrays for electricity generation[J]. *ACS Nano*, 2009, **3**(2): 357 - 362. DOI: 10.1021/nn800804r.

[20] Shao L, Feng P, Liu M, et al. Interface bonding performance and enhancement mechanism of in-situ polymerization modified mortar under wet environments [J]. *Journal of Southeast University* (*Natural Science Edition*), 2023, **53**(5): 749 - 55. DOI: 10.3969/j.issn.1001-505.2023.05.001. (in Chinese)

[21] Xiong Z, Zheng K, Chen Z, et al. Design and mechanical performance analysis of a new GFRP-steel buckling restrained brace [J]. *Journal of Southeast University* (*Natural Science Edition*), 2024, **54**(1): 156 - 166. DOI: 10.3969/j.issn.1001-0505.2024.01.020. (in Chinese)

[22] Du F, She W. Design and fabrication of bioinspired cement aerogel and its performance analysis [J]. *Journal of Southeast University* (*Natural Science Edition*), 2024, **54**(2): 346 - 352. DOI: 10.3969/j.issn.1001-0505.2024.02.011. (in Chinese)

[23] Chang C, Tran V H, Wang J B, et al. Direct-write piezoelectric polymeric nanogenerator with high energy conversion efficiency[J]. *Nano Letters*, 2010, **10**(2): 726 - 731. DOI: 10.1021/nl9040719.

[24] Pu J, Yan X J, Jiang Y D, et al. Piezoelectric actuation of direct-write electrospun fibers[J]. *Sensors and Actuators A*: *Physical*, 2010, **164**(1/2): 131 - 136. DOI: 10.1016/j.sna.2010.09.019.

[25] Fang J, Wang X G, Lin T. Electrical power generator from randomly oriented electrospun poly(vinylidene fluoride) nanofibre membranes [J]. *Journal of Materials Chemistry*, 2011, **21**(30): 11088 - 11091. DOI: 10.1039/C1JM11445J.

[26] Mandal D, Yoon S, Kim K J. Origin of piezoelectricity in an electrospun poly(vinylidene fluoride-trifluoroethylene) nanofiber web-based nanogenerator and nano-pressure sensor[J]. *Macromolecular Rapid Communications*, 2011, **32**(11): 831 - 837. DOI: 10.1002/marc.201100040.

[27] Liu Z H, Pan C T, Lin L W, et al. Piezoelectric properties of PVDF/MWCNT nanofiber using near-field electrospinning[J]. *Sensors and Actuators A*: *Physical*, 2013, **193**: 13 - 24. DOI: 10.1016/j.sna.2013.01.007.

[28] Athira B S, George A, Vaishna Priya K, et al. High-performance flexible piezoelectric nanogenerator based on electrospun PVDF-$BaTiO_3$ nanofibers for self-powered vibration sensing applications[J]. *ACS Applied Materials & Interfaces*, 2022, **14**(39): 44239 - 44250. DOI: 10.1021/acsami.2c07911.

[29] Zhao B B, Chen Z X, Cheng Z F, et al. Piezoelectric nanogenerators based on electrospun PVDF-coated mats composed of multilayer polymer-coated $BaTiO_3$ nanowires [J]. *ACS Applied Nano Materials*, 2022, **5**(6): 8417 - 8428. DOI: 10.1021/acsanm.2c01538.

[30] Liu P, Wu G, Tang B J, et al. Experimental study on mechanical properties of PVDF textile [J]. *Journal of Southeast University* (*Natural Science Edition*), 2017, **47**(6): 1195 - 1200. DOI: 10.3969/j.issn.1001-0505.2017.06.018. (in Chinese)

[31] Chang J, Dommer M, Chang C, et al. Piezoelectric nanofibers for energy scavenging applications[J]. *Nano Energy*, 2012, **1**(3): 356 - 371. DOI: 10.1016/j.nanoen.2012.02.003.

[32] Constantino C J L, Job A E, Simões R D, et al. Phase transition in poly(vinylidene fluoride) investigated with micro-Raman spectroscopy [J]. *Applied Spectroscopy*, 2005, **59**(3): 275 - 279. DOI: 10.1366/0003702053585336.

[33] Mattsson B, Ericson H, Torell L M, et al. Micro-Raman investigations of PVDF-based proton-conducting membranes[J]. *Journal of Polymer Science Part A*: *Polymer Chemistry*, 1999, **37**(16): 3317 - 3327. DOI: 10.1002/(sici)1099-0518(19990815)37: 163317: aid-pola30 > 3.0.co;2-#.

[34] Damaraju S M, Wu S L, Jaffe M, et al. Structural changes in PVDF fibers due to electrospinning and its effect on biological function [J]. *Biomedical Materials*, 2013, **8**(4): 045007. DOI: 10.1088/1748 - 6041/8/4/045007.

[35] Zhou S Y, Zhang H J, Du C Z, et al. Chitosan-doped PVDF film with enhanced electroactive β phase for piezoelectric sensing[J]. *ACS Applied Electronic Materials*, 2024, **6**(4): 2575 - 2583. DOI: 10.1021/acsaelm.4c00184.

[36] Chen J, Wu S, Zhao B, et al. Temperature effect on tensile properties of warp-knitted composite fabric [J]. *Journal of Southeast University* (*Natural Science Edition*), 2020, **50**(2): 251 - 259. DOI: 10.3969/j.issn.1001-505.2020.02.007. (in Chinese)

[37] Bouhamed A, Binyu Q, Böhm B, et al. A hybrid piezoelectric composite flexible film based on PVDF-HFP for boosting power generation [J]. *Compos Sci Technol*, 2021, **208**: 108769. DOI: 10.1016/j.compscitech.

2021.108769.
[38] Wang Y R, Zheng J M, Ren G Y, et al. A flexible piezoelectric force sensor based on PVDF fabrics[J]. *Smart Materials and Structures*, 2011, **20**(4): 045009. DOI: 10.1088/0964-1726/20/4/045009.
[39] Zheng J F, He A H, Li J X, et al. Polymorphism control of poly(vinylidene fluoride) through electrospinning[J]. *Macromolecular Rapid Communications*, 2007, **28**(22): 2159－2162. DOI: 10.1002/marc.200700544.
[40] Ribeiro C, Sencadas V, Ribelles J L G, et al. Influence of processing conditions on polymorphism and nanofiber morphology of electroactive poly(vinylidene fluoride) electrospun membranes[J]. *Soft Materials*, 2010, **8**(3): 274－287. DOI: 10.1080/1539445x.2010.495630.
[41] Liu Z H, Pan C T, Lin L W, et al. Direct-write PVDF nonwoven fiber fabric energy harvesters via the hollow cylindrical near-fieldelectrospinning process[J]. *Smart Materials and Structures*, 2014, **23**(2): 025003. DOI: 10.1088/0964-1726/23/2/025003.
[42] Yu H, Huang T, Lu M X, et al. Enhanced power output of an electrospun PVDF/MWCNTs-based nanogenerator by tuning its conductivity[J]. *Nanotechnology*, 2013, **24**(40): 405401. DOI: 10.1088/0957-4484/24/40/405401.
[43] Uddin A S M I, Lee D, Cho C, et al. Impact of multi-walled CNT incorporation on dielectric properties of PVDF-$BaTiO_3$ nanocomposites and their energy harvesting possibilities[J]. *Coatings*, 2022, **12**(1): 77. DOI: 10.3390/coatings12010077.
[44] Lee J S, Shin K Y, Cheong O J, et al. Highly sensitive and multifunctional tactile sensor using free-standing ZnO/PVDF thin film with graphene electrodes for pressure and temperature monitoring[J]. *Scientific Reports*, 2015, **5**: 7887. DOI: 10.1038/srep07887.
[45] Lee M, Chen C Y, Wang S H, et al. A hybrid piezoelectric structure for wearable nanogenerators[J]. *Advanced Materials*, 2012, **24**(13): 1759－1764. DOI: 10.1002/adma.201200150.
[46] Li Z T, Zhang X, Li G H. In situ ZnO nanowire growth to promote the PVDF piezo phase and the ZnO-PVDF hybrid self-rectified nanogenerator as a touch sensor[J]. *Physical Chemistry Chemical Physics*, 2014, **16**(12): 5475－5479. DOI: 10.1039/c3cp54083a.

静电纺 PVDF 和 $BaTiO_3$ 复合纳米纤维发电装置

周　蕾[1]　周鹤翔[2]　马　建[2,3]

([1] 上海理工大学出版印刷与艺术设计学院, 上海 200093)
([2] 东南大学机械工程学院, 南京 211189)
([3] 东南大学教育部新型光源技术与设备工程研究中心, 南京 211189)

摘要:为提高压电聚合物薄膜的压电性能,研制了聚偏氟乙烯(PVDF)和钛酸钡($BaTiO_3$)纳米颗粒复合压电薄膜,并对其压电性能进行测试.利用静电纺丝工艺,在 15 kV 外置电压条件下制备复合纳米纤维,并使用滚筒收集装置收集纳米纤维薄膜.利用扫描电子显微镜表征纳米纤维结构形貌,采用拉曼光谱测量复合压电薄膜的晶体结构.结果表明,$BaTiO_3$ 纳米颗粒的加入可使复合纳米纤维膜的 β 相增加近 2 倍.与纯静电纺丝 PVDF 压电薄膜相比,添加 $BaTiO_3$ 纳米颗粒的复合压电薄膜压电性显著提高.PVDF 和 $BaTiO_3$ 复合纳米纤维薄膜的最大瞬时开路电压可高达 80 V.

关键词:静电纺丝;聚偏氟乙烯纳米纤维;钛酸钡;压电薄膜
中图分类号:TH789